

Monotone Finite Volume Scheme for Three Dimensional Diffusion Equation on Tetrahedral Meshes

Xiang Lai¹, Zhiqiang Sheng² and Guangwei Yuan^{2,*}

¹ Department of Mathematics, Shandong University, Jinan 250100, P.R. China.

² Laboratory of Computational Physics, Institute of Applied Physics and Computational Mathematics, P.O. Box 8009, Beijing 100088, P.R.China.

Received 22 April 2015; Accepted (in revised version) 9 May 2016

Abstract. We construct a nonlinear monotone finite volume scheme for three-dimensional diffusion equation on tetrahedral meshes. Since it is crucial important to eliminate the vertex unknowns in the construction of the scheme, we present a new efficient eliminating method. The scheme has only cell-centered unknowns and can deal with discontinuous or tensor diffusion coefficient problems on distorted meshes rigorously. The numerical results illustrate that the resulting scheme can preserve positivity on distorted tetrahedral meshes, and also show that our scheme appears to be approximate second-order accuracy for solution.

AMS subject classifications: 65M06, 65M12, 65M55

Key words: Monotonicity, finite volume scheme, diffusion equation, tetrahedral meshes.

1 Introduction

The monotonicity of finite volume scheme is an important issue for accurately and efficiently solving diffusion equations and has been under research for a long time. In the context of anisotropic thermal conduction, the scheme without preserving monotonicity can cause heat to flow from regions of lower temperature to higher temperature, and it can result in negative values of temperature in regions of large temperature variations. The construction of monotone scheme has been an active field of research in recent years.

A new numerical schemes on distorted meshes should satisfy some desirable properties [1], including monotonicity, local conservation, linearity-preserving, stability, high accuracy, and simplicity. To our knowledge, there exists no linear scheme satisfying all the above properties. Usually, a scheme can possess some of the properties mentioned

*Corresponding author. *Email addresses:* qxlai2000@sdu.edu.cn (X. Lai), sheng_zhiqiang@iapcm.ac.cn (Z. Sheng), yuan_guangwei@iapcm.ac.cn (G. Yuan)

above. The classical multi-point flux approximation (MPFA) method [2,3] and nine-point scheme [4–6] are not monotone on general meshes. The schemes in [5,6] consider the case of diffusion coefficient being scalar only. The schemes in [7,8] are monotone under certain severe (geometric) restrictions. The restrictions on monotonicity of the MPFA methods are analyzed in [9–13]. The sufficient condition to ensure the monotonicity of the mimetic finite difference is investigated in [14,15]. Some algorithms in [16] based on slope limiters are proposed to preserve the monotonicity. In [17], based on repair technique and constrained optimization, two approaches have been suggested to enforce discrete extremum principle for linear finite element solutions of general elliptic equations with self-adjoint operator on triangular meshes.

The criteria for the monotonicity of control volume methods on quadrilateral meshes is derived in [10], which shows that it is impossible to construct linear nine-point methods which unconditionally satisfy the monotonicity criteria when the discretization satisfies local conservation and exact reproduction of linear solution.

A few nonlinear finite volume methods with monotonicity have been proposed in [18–22]. It is shown in [18] that the scheme is monotone only for parabolic equations and sufficiently small time steps. Some two-dimensional nonlinear finite volume schemes have been further developed and analyzed in [1], [19–22]. The scheme in [1] is monotone on triangular meshes for strongly anisotropic and heterogeneous full tensor coefficients. Based on an adaptive approach of choosing stencil in the construction of discrete normal flux, a nonlinear finite volume scheme for diffusion problems with anisotropic and heterogeneous full tensor coefficients on arbitrary star-shaped polygonal meshes is proposed in [19]. In [20] a nonlinear finite volume scheme satisfying the discrete extremum principle for diffusion equation on polygonal meshes is constructed. An interpolation-free nonlinear monotone scheme is presented in [21], and it has been extended to the advection diffusion equations on unstructured polygonal meshes in [22].

Up to now there are too many researches on discrete schemes for the two-dimensional diffusion problems. As for the three-dimensional case, there are also some finite volume methods on polyhedral meshes have been discussed, e.g., [23–28]. But monotonicity analysis for them has seldom been studied. An effective way to ensure the monotonicity property is to construct a numerical method such that the final discretization matrix is an M-matrix (see [29]). An M-matrix analysis for three-dimensional schemes, which is the extension of two-dimensional cases in [12,13], has been discussed in [30,31].

In [32] a nonlinear monotone scheme for 3D diffusion problems on unstructured tetrahedral meshes is proposed, which is a generalization of the scheme in [18] on 2D triangular meshes. To construct monotone schemes, the diffusion coefficient and the location of collocation point associated with the cell are restricted. Following the ideas of [19,21], a nonlinear two-point flux approximation scheme is proposed in [33]. The important feature of this method is that most of auxiliary unknowns are interpolated from primary unknowns on the basis of a physical relationship. And it has been extended to the advection diffusion equations on unstructured polyhedral meshes in [34].

In this paper, we develop a nonlinear monotone scheme for three-dimensional dif-

fusion equation on tetrahedral meshes, which uses cell-centered unknowns as primary unknowns. To rigorously deal with discontinuous or tensor diffusion coefficient problems on non-orthogonal meshes, some auxiliary unknowns (e.g., vertex unknowns or edge unknowns) are introduced in addition to the primary unknowns. Our main contribution is that an efficient method to eliminate the vertex unknowns is constructed and the computational cost is remarkably reduced. We exploit a feature of the nonlinear monotone scheme that the vertex unknowns appear only in the coefficient matrix, so they can be taken as the values at previous nonlinear iteration step. It follows that at each vertex we avoid solving a local system with both auxiliary and primary unknowns, otherwise it increases computational cost greatly. The construction of the scheme can be easily to extend to more general polyhedral meshes, but the description of the scheme becomes somewhat complicated in this case, so we will focus on tetrahedral meshes.

The rest of this paper is organized as follows. In Section 2, The construction of a nonlinear scheme is presented. In Section 3, a new method is proposed to eliminate the vertex unknowns. And in Section 4, Picard iteration for solving the nonlinear discrete system, and the monotonicity theorem are given. In Section 5, several numerical examples are given to illustrate the performance of the scheme and the convergence rate of the scheme is also presented.

2 Construction of monotone nonlinear scheme

2.1 Problem and notation

Consider the stationary diffusion problem with a Dirichlet boundary condition

$$-\nabla \cdot (\kappa \nabla u) = f \quad \text{in } \Omega, \quad (2.1)$$

$$u(x) = g \quad \text{on } \partial\Omega, \quad (2.2)$$

where Ω is an open bounded set of R^3 with boundary $\partial\Omega$, and $\kappa = \kappa(x)$ is a diffusion tensor, which is essentially bounded and positive definite, i.e., there exist two positive constants κ_- and κ_+ such that, for any $x \in \Omega$ and all $\xi \in R^3$, $\kappa_- |\xi|^2 \leq \kappa(x) \xi \cdot \xi \leq \kappa_+$.

In this paper, we use a mesh on Ω made up of tetrahedron and denote the neighboring cells by K and L . With each cell K we associate one point denoted also by K : the barycenter is a qualified candidate but other points can also be chosen.

Denote the cell-vertices by $Q_1, Q_2, Q_3, Q_4, \dots$, and the cell face by S . $|S|$ is the area of S . If the cell face S is a common face of cells K and L , then denote $S = K|L$. Denote \mathbf{n}_{KS} (resp. \mathbf{n}_{LS}) as the unit outer normal vector on the face S of cell K (resp. L). Then $\mathbf{n}_{KS} = -\mathbf{n}_{LS}$ holds for $S = K|L$. Denote \mathbf{t}_{KQ_i} (reps. \mathbf{t}_{LQ_i}) be the unit tangential vector on the lines KQ_i (resp. LQ_i) ($i = 1, 2, \dots$), respectively.

Let \mathcal{J} be the set of all cells, ε be the set of all cell-faces, and ε_K be the set of all cell-faces of cell K . Denote $\varepsilon_{int} = \varepsilon \cap \Omega$, $\varepsilon_{ext} = \varepsilon \cap \partial\Omega$, and $m(K)$ be the volume of cell K .

Let κ^T be the transpose of matrix κ . Discrete stencil and some notations are shown in Fig. 1. The ray originated in the point K along $\kappa^T \mathbf{n}_{KS}$ must intersect one of the cell-face

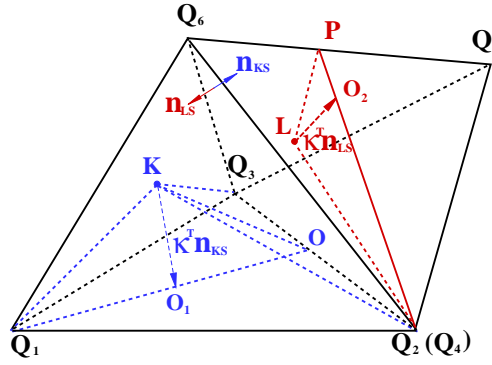


Figure 1: Stencil and notation.

of cell K , and this cell-face is denoted as $Q_1Q_2Q_3$, and the intersection point is O_1 . Q_1O_1 intersects Q_2Q_3 at point O . Similarly, the ray originated in the point L along $\kappa^T \mathbf{n}_{LS}$ must intersect one of the cell-face of cell L , and this cell-face is denoted as $Q_4Q_5Q_6$, and the intersection point is O_2 . Q_4O_2 intersects Q_5Q_6 at the point P .

2.2 Construction of scheme

Integrate (2.1) over the cell K to obtain

$$\sum_{S \in \mathcal{E}_K} \mathcal{F}_{K,S} = \int_K f(x) dx,$$

where the continuous flux on the cell face S is

$$\mathcal{F}_{K,S} = - \iint_S \kappa \nabla u \cdot \mathbf{n}_{KS} dS = - \iint_S \nabla u \cdot \kappa^T \mathbf{n}_{KS} dS. \tag{2.3}$$

Since KQ_1, KQ_2 and KQ_3 are the three edges of tetrahedron $KQ_1Q_2Q_3$ sharing one point K (see Fig. 1), the unit tangential vectors $\mathbf{t}_{KQ_1}, \mathbf{t}_{KQ_2}$ and \mathbf{t}_{KQ_3} cannot be coplanar. Then there exist three scalars a_1, b_1 and c_1 such that

$$\kappa^T \mathbf{n}_{KS} = a_1 \mathbf{t}_{KQ_1} + b_1 \mathbf{t}_{KQ_2} + c_1 \mathbf{t}_{KQ_3},$$

where

$$a_1 = \frac{(\kappa^T(K) \mathbf{n}_{KS}, \mathbf{n}_{KQ_3Q_2})}{(\mathbf{t}_{KQ_1}, \mathbf{n}_{KQ_3Q_2})}, \quad b_1 = \frac{(\kappa^T(K) \mathbf{n}_{KS}, \mathbf{n}_{KQ_1Q_3})}{(\mathbf{t}_{KQ_2}, \mathbf{n}_{KQ_1Q_3})}, \quad c_1 = \frac{(\kappa^T(K) \mathbf{n}_{KS}, \mathbf{n}_{KQ_2Q_1})}{(\mathbf{t}_{KQ_3}, \mathbf{n}_{KQ_2Q_1})},$$

and $\mathbf{n}_{KQ_3Q_2}$ is the unit outer normal vector on the face KQ_3Q_2 , and $\mathbf{n}_{KQ_1Q_3}$ and $\mathbf{n}_{KQ_2Q_1}$ have similar meaning. From (2.3), we have

$$\mathcal{F}_{K,S} = -|S| \left(a_1 \frac{u_{Q_1} - u_K}{|KQ_1|} + b_1 \frac{u_{Q_2} - u_K}{|KQ_2|} + c_1 \frac{u_{Q_3} - u_K}{|KQ_3|} \right) + \mathcal{O}(h^3).$$

Let $F_{K,S}$ be the discrete normal flux on the face S of cell K , then

$$F_{K,S} = -|S| \left(a_1 \frac{u_{Q_1} - u_K}{|KQ_1|} + b_1 \frac{u_{Q_2} - u_K}{|KQ_2|} + c_1 \frac{u_{Q_3} - u_K}{|KQ_3|} \right).$$

Similarly, the discrete normal flux on the face S of cell L is defined as:

$$F_{L,S} = -|S| \left(a_2 \frac{u_{Q_4} - u_L}{|LQ_4|} + b_2 \frac{u_{Q_5} - u_L}{|LQ_5|} + c_2 \frac{u_{Q_6} - u_L}{|LQ_6|} \right),$$

where

$$a_2 = \frac{(\kappa^T(L)\mathbf{n}_{LS}, \mathbf{n}_{KQ_6Q_5})}{(\mathbf{t}_{KQ_4}, \mathbf{n}_{KQ_6Q_5})}, \quad b_2 = \frac{(\kappa^T(L)\mathbf{n}_{LS}, \mathbf{n}_{KQ_4Q_6})}{(\mathbf{t}_{KQ_5}, \mathbf{n}_{KQ_4Q_6})}, \quad c_2 = \frac{(\kappa^T(L)\mathbf{n}_{LS}, \mathbf{n}_{KQ_5Q_4})}{(\mathbf{t}_{KQ_6}, \mathbf{n}_{KQ_5Q_4})}.$$

By the continuity of the normal flux component $F_{K,S} = -F_{L,S}$, we define

$$F_{K,S} = -\mu_1 |S| \left(a_1 \frac{u_{Q_1} - u_K}{|KQ_1|} + b_1 \frac{u_{Q_2} - u_K}{|KQ_2|} + c_1 \frac{u_{Q_3} - u_K}{|KQ_3|} \right) + \mu_2 |S| \left(a_2 \frac{u_{Q_4} - u_L}{|LQ_4|} + b_2 \frac{u_{Q_5} - u_L}{|LQ_5|} + c_2 \frac{u_{Q_6} - u_L}{|LQ_6|} \right),$$

where μ_1 and μ_2 are some coefficients to be determined. $F_{K,S}$ can be rewritten as

$$F_{K,S} = \mu_1 |S| \left(\frac{a_1}{|KQ_1|} + \frac{b_1}{|KQ_2|} + \frac{c_1}{|KQ_3|} \right) u_K - \mu_2 |S| \left(\frac{a_2}{|LQ_4|} + \frac{b_2}{|LQ_5|} + \frac{c_2}{|LQ_6|} \right) u_L - \mu_1 \alpha_1 + \mu_2 \alpha_2, \quad (2.4)$$

where

$$\alpha_1 = |S| \left(\frac{a_1}{|KQ_1|} u_{Q_1} + \frac{b_1}{|KQ_2|} u_{Q_2} + \frac{c_1}{|KQ_3|} u_{Q_3} \right),$$

$$\alpha_2 = |S| \left(\frac{a_2}{|LQ_4|} u_{Q_4} + \frac{b_2}{|LQ_5|} u_{Q_5} + \frac{c_2}{|LQ_6|} u_{Q_6} \right).$$

In order to obtain the two-point flux approximation, the third and the fourth terms at the right of Eq. (2.4) should be vanished. Hence μ_1 and μ_2 should satisfy

$$\begin{cases} \mu_1 + \mu_2 = 1, \\ -\alpha_1 \mu_1 + \alpha_2 \mu_2 = 0. \end{cases} \quad (2.5)$$

If $\alpha_1 + \alpha_2 \neq 0$, then $\mu_1 = \frac{\alpha_2}{\alpha_1 + \alpha_2}$, $\mu_2 = \frac{\alpha_1}{\alpha_1 + \alpha_2}$. If $\alpha_1 + \alpha_2 = 0$, then $\mu_1 = \mu_2 = \frac{1}{2}$.

For $S = K|L \in \varepsilon_{int}$, by (2.4) and (2.5), we have

$$\begin{aligned}
 F_{K,S} &= \mu_1 |S| \left(\frac{a_1}{|KQ_1|} + \frac{b_1}{|KQ_2|} + \frac{c_1}{|KQ_3|} \right) u_K \\
 &\quad - \mu_2 |S| \left(\frac{a_2}{|LQ_4|} + \frac{b_2}{|LQ_5|} + \frac{c_2}{|LQ_6|} \right) u_L \\
 &= A_{K,S} u_K - A_{L,S} u_L,
 \end{aligned} \tag{2.6}$$

where

$$\begin{aligned}
 A_{K,S} &= \mu_1 |S| \left| \kappa^T(K) \mathbf{n}_{KS} \right| \frac{1}{|KO_1|}, \\
 A_{L,S} &= \mu_2 |S| \left| \kappa^T(L) \mathbf{n}_{LS} \right| \frac{1}{|LO_2|}.
 \end{aligned}$$

In (2.6), if Q_i lies on $\partial\Omega$, then we take $u_{Q_i} = g(Q_i)$ in the corresponding formula. With the definition of $F_{K,S}$, the finite volume scheme is constructed as follows:

$$\sum_{S \in \varepsilon_K} F_{K,S} = f_K m(K), \quad \forall K \in \mathcal{J}, \tag{2.7}$$

$$u_{Q_i} = g(Q_i), \quad \forall Q_i \in \partial\Omega, \tag{2.8}$$

where $f_K = f(K)$.

The cell center can be collocated at any position of the cell in above scheme. And the coefficients $A_{K,S}$ and $A_{L,S}$ depend on the cell vertex unknowns, hence this scheme is nonlinear.

3 The approximation of cell vertex unknowns

From the above discussion, we know that the flux depends on the vertex unknowns in addition to cell-centered unknowns. Now we will consider how to eliminate the vertex unknowns locally, or approximate the vertex unknowns by certain combination of neighboring cell-centered unknowns.

In [4, 6, 19] some methods are given to eliminate the vertex unknowns for 2D problems. These methods cannot be directly extended to three-dimensional problems. In [30], each vertex unknown can be eliminated by solving a linear system. However in solving three-dimensional problems too much time is needed by this method. So a new efficient method should be proposed to eliminate the vertex unknowns for three-dimensional problems.

In order to obtain the expression of the vertex unknown u_Q , we first construct a control volume around vertex Q . Suppose that there are N tetrahedra surrounding the vertex Q . In each tetrahedron, we connect the midpoints A, B, C of the three edges sharing Q , to

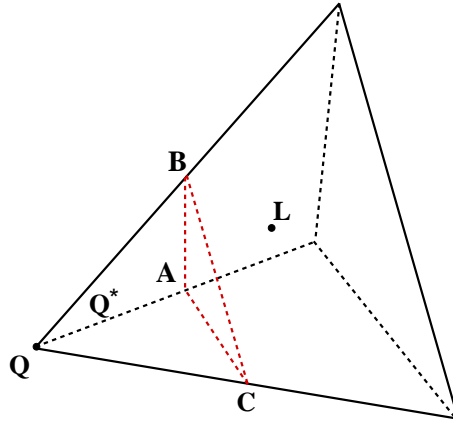


Figure 2: The control volume of vertex Q.

obtain a tetrahedral region $QABC$ (see Fig. 2). Then the control volume of Q , denoted as Q^* , is formed. It is obvious that Q^* is a N -faced polyhedron.

Suppose that L is the cell around Q . Denote the face $S' = \triangle ABC$. Let \mathcal{G}_Q be the set of all the faces S' of Q^* . Denote $\mathbf{n}_{QS'}$ (resp. $\mathbf{n}_{LS'}$) as the unit outer normal vector on the face S' of Q^* (resp. L). Then $\mathbf{n}_{QS'} = -\mathbf{n}_{LS'}$ holds for S' .

Define $u^- = u|_{Q^*}, u^+ = u|_{L \setminus QABC}$, and similarly define κ^-, κ^+ . Moreover, denote $\lambda^- = |(\kappa^-)^T \mathbf{n}_{QS'}|, \lambda^+ = |(\kappa^+)^T \mathbf{n}_{LS'}|$.

The ray originated in the vertex Q along $(\kappa^-)^T \mathbf{n}_{QS'}$ intersects the plane that is generated by the cell face S' , and the intersection point is denoted by Q' . Similarly, the ray originated in the point L along $(\kappa^+)^T \mathbf{n}_{LS'}$ intersects the plane generated by the face S' , and the intersection point is L' . The point I is any given point on face S' (see Fig. 3).

In order to obtain the vertex unknown u_Q , we adopt the diamond scheme in [28] on the control volume Q^* , which will be described briefly for completeness. Let's see Fig. 2 and Fig. 3. Now, the discrete normal flux on the face ABC is constructed by a linear combination of the directional flux along the line connecting the vertex Q and the cell-center L and the tangent flux along the cell-faces (S').

From Fig. 3, we know that

$$\frac{(\kappa^-)^T \mathbf{n}_{QS'}}{|(\kappa^-)^T \mathbf{n}_{QS'}|} = \frac{\mathbf{QQ}'}{|\mathbf{QQ}'|}, \quad \frac{(\kappa^+)^T \mathbf{n}_{LS'}}{|(\kappa^+)^T \mathbf{n}_{LS'}|} = \frac{\mathbf{LL}'}{|\mathbf{LL}'|}.$$

Since

$$\mathbf{QQ}' = \mathbf{QI} + \mathbf{IQ}'$$

we have

$$\nabla u^-(I) \cdot \mathbf{QQ}' = \nabla u^-(I) \cdot \mathbf{QI} + \nabla u^-(I) \cdot \mathbf{IQ}'.$$

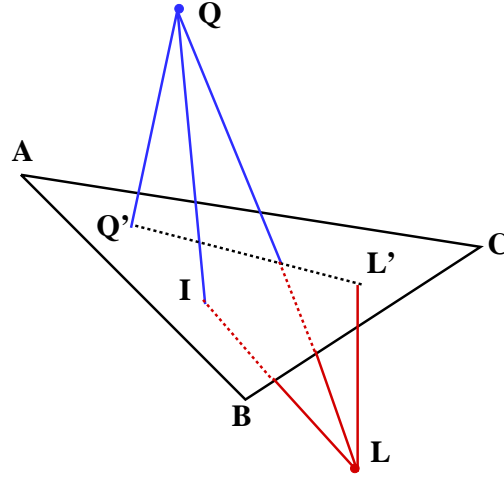


Figure 3: Stencil and notation of vertex Q.

Then

$$\begin{aligned} \kappa^- \nabla u^-(I) \cdot \mathbf{n}_{QS'} &= \frac{\lambda^-}{|\mathbf{QQ}'|} \nabla u^-(I) \cdot \mathbf{QI} + \frac{\lambda^-}{|\mathbf{QQ}'|} \nabla u^-(I) \cdot \mathbf{IQ}' \\ &\approx \frac{\lambda^-}{|\mathbf{QQ}'|} (u_I - u_Q) + \frac{\lambda^-}{|\mathbf{QQ}'|} \nabla u^-(I) \cdot \mathbf{IQ}'. \end{aligned} \quad (3.1)$$

Similarly,

$$\begin{aligned} \kappa^+ \nabla u^+(I) \cdot \mathbf{n}_{LS'} &= \frac{\lambda^+}{|\mathbf{LL}'|} \nabla u^+(I) \cdot \mathbf{LI} + \frac{\lambda^+}{|\mathbf{LL}'|} \nabla u^+(I) \cdot \mathbf{IL}' \\ &\approx \frac{\lambda^+}{|\mathbf{LL}'|} (u_I - u_L) + \frac{\lambda^+}{|\mathbf{LL}'|} \nabla u^+(I) \cdot \mathbf{IL}'. \end{aligned} \quad (3.2)$$

From the continuity of the normal flux,

$$\kappa^- \nabla u^-(I) \cdot \mathbf{n}_{QS'} = -\kappa^+ \nabla u^+(I) \cdot \mathbf{n}_{LS'},$$

it follows that

$$u_I = \frac{1}{a+b} [au_Q + bu_L - b \nabla u^+ \cdot \mathbf{IL}' - a \nabla u^- \cdot \mathbf{IQ}'],$$

where $a = \frac{\lambda^-}{|\mathbf{QQ}'|}$, $b = \frac{\lambda^+}{|\mathbf{LL}'|}$. We know that the tangent derivative of u on S is continuous, i.e.,

$$\nabla u^- \cdot \mathbf{t} = \nabla u^+ \cdot \mathbf{t}, \forall \mathbf{t} \perp \mathbf{n}_{QS'}, \text{ on } S',$$

hence

$$\begin{aligned} \kappa^- \nabla u^-(I) \cdot \mathbf{n}_{QS'} &= a(u_I - u_Q) + a \nabla u(I) \cdot \mathbf{IQ}' \\ &= \frac{ab}{a+b} [-u_Q + u_L] + \nabla u \cdot \left[-\frac{ab}{a+b} \mathbf{IL}' + a \mathbf{IQ}' - \frac{a^2}{a+b} \mathbf{IQ}' \right]. \end{aligned} \quad (3.3)$$

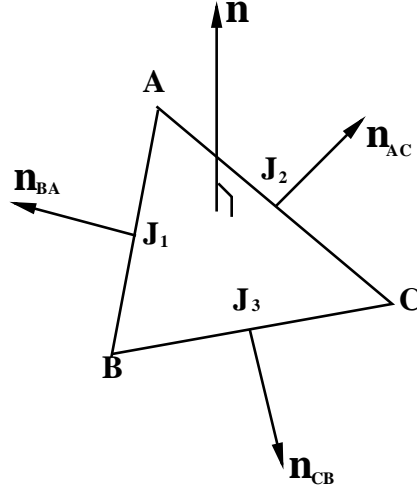


Figure 4: The face stencil.

Also, there holds

$$\mathbf{I}\mathbf{Q}' = \mathbf{I}\mathbf{L}' + \mathbf{L}'\mathbf{Q}',$$

and then

$$\lambda^- \nabla u^-(I) \cdot \mathbf{n}_{QS'} = \frac{ab}{a+b} [-u_Q + u_L - \nabla u \cdot \mathbf{Q}'\mathbf{L}'].$$

It follows that the discrete normal flux on S' is

$$\begin{aligned} F_{Q,S'} &= -\kappa^- \nabla u^-(I) \cdot \mathbf{n}_{QS'} |S'| \\ &= \frac{\lambda^+ \lambda^- |S'|}{\lambda^+ |QQ'| + \lambda^- |LL'|} [u_Q - u_L + \nabla u \cdot \mathbf{Q}'\mathbf{L}']. \end{aligned} \quad (3.4)$$

Now we approximate ∇u on the face $S' = \triangle ABC$ as follows.

$$\begin{aligned} \nabla u &= \frac{1}{|\triangle ABC|} \int_{\triangle ABC} \nabla u = \frac{1}{|\triangle ABC|} \int_{\partial \triangle ABC} u \mathbf{n} dl \\ &\approx \frac{1}{|\triangle ABC|} (u_{J_1} \mathbf{n}_{BA} + u_{J_2} \mathbf{n}_{AC} + u_{J_3} \mathbf{n}_{CB}) \\ &\approx -\frac{1}{2|\triangle ABC|} (u_A \mathbf{n}_{CB} + u_B \mathbf{n}_{AC} + u_C \mathbf{n}_{BA}), \end{aligned} \quad (3.5)$$

where J_1, J_2 and J_3 are the midpoints of the edge BA, AC and CB respectively. Moreover the midpoints formulae, e.g., $u_{J_1} = \frac{1}{2}(u_A + u_B)$, have been used. And $\mathbf{n}_{AC} = \mathbf{n} \times \mathbf{AC}, \mathbf{n}_{CB} = \mathbf{n} \times \mathbf{CB}, \mathbf{n}_{BA} = \mathbf{n} \times \mathbf{BA}$, and \mathbf{n} is the unit normal vector to $\triangle ABC$ (see Fig. 4).

Substituting (3.5) into (3.4), we obtain

$$F_{Q,S'} = \frac{\lambda^- \lambda^+ |S'|}{\lambda^+ |QQ'| + \lambda^- |LL'|} \left[(u_Q - u_L) - \frac{(u_A \mathbf{n}_{CB} + u_B \mathbf{n}_{AC} + u_C \mathbf{n}_{BA}) \cdot \mathbf{Q}'\mathbf{L}'}{2|S'|} \right]. \quad (3.6)$$

Note that A, B, C are the midpoints of edge of cell L , so u_A, u_B, u_C can be expressed by the arithmetic average of corresponding vertex unknowns of cell L . Let \mathcal{G}_Q be the set of all the cell-faces S' of Q^* and $\tilde{\mathcal{J}}$ the set of all vertices. Then $\{u_Q\}$ satisfy

$$\sum_{S' \in \mathcal{G}_Q} F_{Q,S'} = f(Q)m(Q), \quad \forall Q \in \tilde{\mathcal{J}}. \tag{3.7}$$

Actually this is a coupled system of vertex unknowns and cell-centered unknowns. Fortunately, we need not to solve this system of equations, since the vertex unknowns appear only in the coefficients $A_{K,S}$ and $A_{L,S}$ in the flux equation (2.6), and when Picard iteration is applied to solve (2.7)-(2.8) (see the next section), we need only the vertex-unknown values at previous iteration step. Thus, let k be the iteration index and

$$F_{Q,S'}^{(k+1)} = \frac{\lambda^- \lambda^+ |S'|}{\lambda^+ |\mathbf{Q}\mathbf{Q}'| + \lambda^- |\mathbf{L}\mathbf{L}'|} \left[(u_Q^{(k+1)} - u_L^{(k)}) - \frac{(u_A^{(k)} \mathbf{n}_{CB} + u_B^{(k)} \mathbf{n}_{AC} + u_C^{(s)} \mathbf{n}_{BA}) \cdot \mathbf{Q}'\mathbf{L}'}{2|S'|} \right]. \tag{3.8}$$

Then $u_Q^{(k+1)}$ is obtained by the following formula

$$\sum_{S' \in \mathcal{G}_Q} F_{Q,S'}^{(k+1)} = f(Q)m(Q), \quad \forall Q \in \tilde{\mathcal{J}}. \tag{3.9}$$

So the vertex unknowns of the $(k+1)$ -th iteration step are expressed by the combination of cell-centered unknowns and the midpoint unknowns of the (k) -th iteration step. This method can deal with both continuous and discontinuous coefficient problems. Moreover, because the vertex unknowns can be eliminated without solving linear systems, the computation cost is reduced remarkably.

4 Discrete system, Picard iteration and monotonicity

Substituting (2.6) into (2.7), we obtain a nonlinear algebraic system:

$$A(U)U = F, \tag{4.1}$$

where U is the vector discrete unknowns,

$$A(U) = \sum_{S \in \mathcal{E}} N_S A_S(U) N_S^T$$

is represented by assembling of 2×2 matrices

$$A_S(U) = \begin{pmatrix} A_{K,S}(U) & -A_{L,S}(U) \\ -A_{K,S}(U) & A_{L,S}(U) \end{pmatrix}$$

for interior faces and 1×1 matrices $A_S(U) = A_{K,S}(U)$ for boundary faces. N_S are assembling matrices consisting of zeros and ones.

The Picard iteration is employed to solve the nonlinear system (4.1). That is: Choose a small value $\varepsilon_{non} > 0$ and initial cell-centered vector $U^{(0)} \geq 0$, initial vertices vector $V^{(0)} \geq 0$, and repeat for $k=1, 2, \dots$,

1. Using $U^{(k-1)}, V^{(k-1)}$ and Eqs. (3.8), (3.9), to calculate $V^{(k)}$.
2. Using $V^{(k-1)}$ to calculate $A(U^{(k-1)})$ and solve $A(U^{(k-1)})U^{(k)} = F$.
3. Using $V^{(k)}$ to calculate $A(U^{(k)})$ and stop if

$$\|A(U^{(k)})U^{(k)} - F\| \leq \varepsilon_{non} \|A(U^{(0)})U^{(0)} - F\|.$$

In our numerical experiments, we take $\varepsilon_{non} = 1.0e^{-6}$.

The matrix $A(U)$ is non-symmetric and has the following properties:

1. All diagonal entries of matrix $A(U)$ are positive;
2. All off-diagonal entries of $A(U)$ are non-positive;
3. Each column sum in $A(U)$ is non-negative and there exists a column with a positive sum.

Note that the coefficients $A_{K,S}$ and $A_{L,S}$ in (2.6) are non-negative provide that the vertex unknowns are non-negative. The proof of monotonicity is the same as that in [19]. Here we only give the following theorem.

Theorem 4.1. *Assume that $F \geq 0$, $U^{(0)} \geq 0$, and the vertex unknowns are non-negative, and linear systems in Picard iterations are solved exactly. Then all iterations $U^{(k)}$ are non-negative vectors:*

$$U^{(k)} \geq 0, \quad k=1, 2, \dots.$$

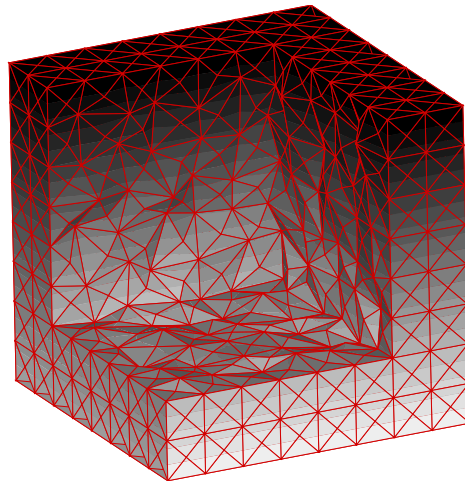
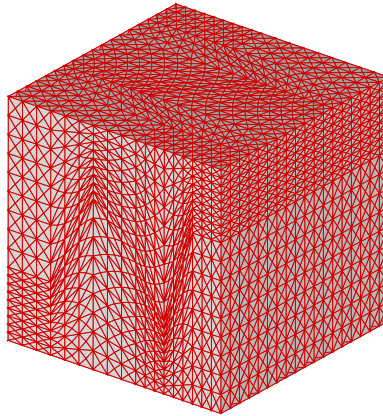
5 Numerical experiments

The discrete L_2 -norms is used to evaluate approximation errors. For the solution u , the following L_2 -norm is applied:

$$\varepsilon_2^u = \left[\sum_{K \in \mathcal{J}} (u_K - u(K))^2 m(K) \right]^{\frac{1}{2}}.$$

For the flux F , we use the following L_2 -norm:

$$\varepsilon_2^F = \left[\sum_{S \in \varepsilon} (F_{K,S} - \mathcal{F}_{K,S})^2 \right]^{\frac{1}{2}}.$$

Figure 5: Mesh A: a random tetrahedra meshes ($h=1/8$).Figure 6: Mesh B: random tetrahedra meshes generated from Kershaw grid ($h=1/18$).

We construct two mesh partitions: one is that we take a uniform cubic partition on $\Omega = [0,1]^3$ with a mesh size h , split each cube into 24 random tetrahedra with randomly distorted position of mesh nodes:

$$\begin{aligned} X &= x + \xi_x h, \\ Y &= y + \xi_y h, \\ Z &= z + \xi_z h, \end{aligned}$$

where ξ_x , ξ_y and ξ_z are random variables with values between -0.3 and 0.3 (see Fig. 5). The other is that we take a three dimensional trapezoidal grid like Kershaw mesh on $\Omega = [0,1]^3$ with a mesh size h , then split each trapezoidal mesh into 24 tetrahedra. We call the first kind mesh A, the second kind mesh B (see Fig. 6).

In the following, we firstly give a numerical example to test the positivity of numerical solution of our scheme. Then we give some numerical tests to demonstrate the accuracy of the discrete scheme. For all the examples, the method in section 3 is applied to eliminate the vertex unknowns.

5.1 Positivity of numerical solutions

Consider the problem (2.1)-(2.2) in unit cube $\Omega = [0,1]^3$ with

$$\kappa = \begin{pmatrix} y^2 + \varepsilon x^2 & -(1-\varepsilon)xy & 0 \\ -(1-\varepsilon)xy & x^2 + \varepsilon y^2 & 0 \\ 0 & 0 & 1 \end{pmatrix}, \quad \varepsilon = 5 \times 10^{-3}, \quad (5.1)$$

and

$$f = \begin{cases} 1, & \text{if } (x,y) \in [\frac{3}{8}, \frac{5}{8}]^2, z \in [0,1], \\ 0, & \text{otherwise.} \end{cases}$$

The homogeneous Dirichlet boundary condition is imposed on $\partial\Omega$.

The exact solution $u(x,y,z)$ is unknown, but the maximum principle states that it is non-negative. Yuan and Sheng in [19] discussed a similar two-dimensional problem with (5.1). They illustrated that the numerical solutions obtained by MPFA has non-physical oscillations, and MPFA can produce negative values. We test our nonlinear finite volume schemes on uniform and random tetrahedral meshes. The numerical results obtained on different meshes are shown in Tables 1 and 2, which demonstrate that our scheme preserves positivity of the numerical solution.

Table 1: The numerical solution on uniform tetrahedral meshes.

Mesh size	Number of iteration	u_{\min}	u_{\max}
1/8	13	2.16e-13	5.25e-02
1/16	25	1.13e-16	5.69e-02
1/32	44	1.11e-19	5.89e-02
1/64	91	1.91e-22	5.98e-02

Table 2: The numerical solution on random tetrahedral meshes.

Mesh size	Number of iteration	u_{\min}	u_{\max}
1/8	16	7.18e-15	4.99e-02
1/16	31	1.80e-15	5.59e-02
1/32	55	1.15e-16	5.87e-02
1/64	116	9.50e-18	5.94e-02

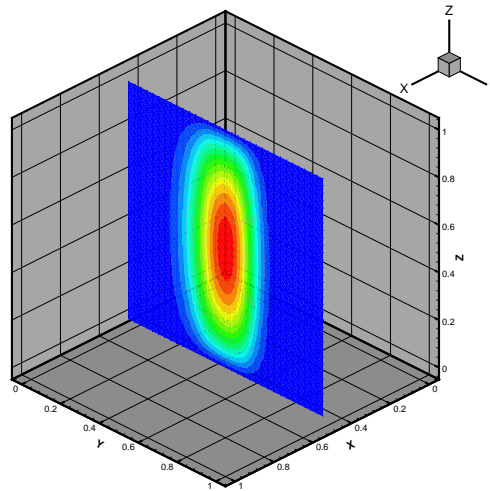


Figure 7: The slice of numerical solution at $x=0.5$ on uniform tetrahedral meshes.

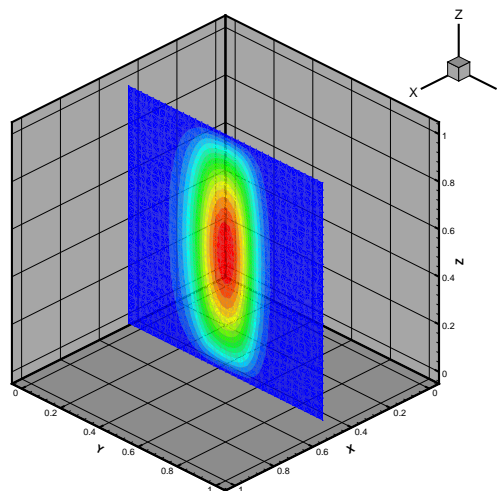


Figure 8: The slice of numerical solution at $x=0.5$ on random tetrahedral meshes.

Let \mathcal{J}' be internal tetrahedral cells in Ω . Denote

$$u_{\min} = \min_{K \in \mathcal{J}'} u_K, \quad u_{\max} = \max_{K \in \mathcal{J}} u_K.$$

From Tables 1 and 2, one can see that the minimum value of numerical solutions is positive and close to zero. Hence the non-negative discrete solutions are obtained by our method. Figs. 7 and 8 give the slice of numerical solution at $x = 0.5$ on uniform and random tetrahedral meshes ($h = 1/32$) respectively.

5.2 Scalar diffusion coefficient

Consider the problem (2.1)-(2.2) with Dirichlet boundary condition in the unit cube $\Omega = [0,1]^3$.

Let $\kappa(x,y,z) = 1+x+y+z$. The solution is chosen to be $u = \sin(\pi x)\sin(\pi y)\sin(\pi z)$. Then the corresponding function

$$f = 3\pi^2\kappa(x,y,z)\sin(\pi x)\sin(\pi y)\sin(\pi z) - \pi(\cos(\pi x)\sin(\pi y)\sin(\pi z) + \sin(\pi x)\cos(\pi y)\sin(\pi z) + \sin(\pi x)\sin(\pi y)\cos(\pi z)),$$

and $g=0$.

Tables 3 and 4 give the errors between exact solutions and numerical solutions on tetrahedral mesh A and B, respectively. From Table 3 and Table 4, one can see that, on meshes A and B, the convergent order for the solution is almost second order.

Table 3: Numerical results for scalar diffusion coefficient on mesh A.

The number of cell	24×6^3	24×12^3	24×18^3	24×24^3
Mesh size(h)	1/6	1/12	1/18	1/24
ε_2^u	2.80e-3	6.62e-4	3.05e-4	1.74e-4
Rate	2.01	1.91	1.95

Table 4: Numerical results for scalar diffusion coefficient on mesh B.

The number of cell	24×6^3	24×12^3	24×18^3	24×24^3
Mesh size(h)	1/6	1/12	1/18	1/24
ε_2^u	6.94e-3	2.60e-3	1.30e-3	7.35e-4
Rate	1.42	1.71	1.98

5.3 Full anisotropic tensor

Consider the problem (2.1)-(2.2) with Dirichlet boundary condition in the unit cube $\Omega = [0,1]^3$.

Let κ be the symmetric positive definite matrix defined by

$$\kappa = \begin{pmatrix} 1 & 0 & 0 \\ 0 & 1 & 0 \\ 0 & 0 & 1000 \end{pmatrix}.$$

The solution is chosen to be $u = 1+x-y^2+z$, the corresponding function

$$f = 2.0.$$

It shows in Tables 5 and 6 that the method is almost second order convergence for the solution.

Table 5: Numerical results for full anisotropic tensor on mesh A.

The number of cell	24×6^3	24×12^3	24×18^3	24×24^3
Mesh size(h)	1/6	1/12	1/18	1/24
ϵ_2^u	1.61e-3	4.63e-4	2.25e-4	1.36e-4
Rate	1.80	1.78	1.77

Table 6: Numerical results for full anisotropic tensor on mesh B.

The number of cell	24×6^3	24×12^3	24×18^3	24×24^3
Mesh size(h)	1/6	1/12	1/18	1/24
ϵ_2^u	1.69e-3	4.13e-4	1.86e-4	1.05e-4
Rate	2.03	1.97	2.01

5.4 Discontinuous diffusion coefficient

When κ is discontinuous scalar, we consider problem (2.1)-(2.2) with Dirichlet boundary condition. Let

$$\kappa = \begin{cases} 5.0, & x \leq 0.5, \\ 1.0, & x > 0.5. \end{cases}$$

The exact solution is

$$u = \begin{cases} \sin \pi x + e^y + z, & x \leq 0.5, \\ \sin 5\pi x + e^y + z, & x > 0.5. \end{cases}$$

then

$$f = \begin{cases} 5\pi^2 \sin \pi x - 5e^y, & x \leq 0.5, \\ 25\pi^2 \sin 5\pi x - e^y, & x > 0.5. \end{cases}$$

This solution and its normal component of flux are continuous at $x = \frac{1}{2}$.

Table 7 and Table 8 show that the convergent rate for solution is almost second order.

From these experiments, we can see that our method is robust to deal with the cases that κ is continuous and discontinuous.

Table 7: Convergence results for discontinuous problem on mesh A.

The number of cell	24×6^3	24×12^3	24×18^3	24×24^3
Mesh size(h)	1/6	1/12	1/18	1/24
ϵ_2^u	6.89e-2	1.38e-2	6.13e-3	3.37e-3
Rate	2.32	2.00	2.08

Table 8: Convergence results for discontinuous problem on mesh B.

The number of cell	24×6^3	24×12^3	24×18^3	24×24^3
Mesh size(h)	1/6	1/12	1/18	1/24
ε_2^u	5.98e-2	1.27e-2	5.60e-3	3.14e-3
Rate	2.23	2.01	2.02

5.5 Vertex-unknown elimination method and computation cost

We give an example to illustrate the influence of the vertex-unknown elimination method on the computation time.

We consider a problem (2.1)-(2.2) with Dirichlet boundary condition and κ being discontinuous as follows

$$\kappa = \begin{cases} 4.0, & x \leq 0.5, \\ 1.0, & x > 0.5. \end{cases}$$

The exact solution is

$$u = \begin{cases} 2 + x + y + z, & x \leq 0.5, \\ 0.5 + 4x + y + z, & x > 0.5. \end{cases}$$

And

$$f = 0.$$

Denote the method of eliminating the vertex unknowns proposed in [19] as (A), and the iteration method in section 3 as (B). In the method (A), an under-determined system for each vertex unknown should be solved. Similar method is also proposed in [30]. In the methods (B) vertex unknowns are computed directly, which hardly takes time. So the time cost only with the method (A) is shown in Table 9.

Table 9: Computation cost with method (A).

The number of cell	24×6^3	24×12^3	24×18^3	24×24^3	24×32^3
Mesh size(h)	1/6	1/12	1/18	1/24	1/32
time(s)	0	4	44	242	1069

From Table 9, we can see that the time cost increases intolerably as mesh size decreasing by the method (A) of solving a local linear system. So we should try our best to avoid solving local linear systems in eliminating vertex unknowns.

6 Conclusion

In this paper a nonlinear monotone finite volume scheme is constructed for solving three-dimensional diffusion equation with scalar or full anisotropic symmetric tensor coefficients on tetrahedral meshes. The discretization stencil is chosen to adapt to geometry of

distorted mesh. Compared with two-dimensional problem, it is more difficult to eliminate the vertex unknowns for three-dimensional problem. We present a new method of eliminating the vertex unknowns for three-dimensional problem, which does not need to solve the linear system, so the computation cost is reduced remarkably. Numerical experiments are presented to show the positivity and accuracy of the monotone scheme, and the efficiency of the vertex-unknown elimination methods.

Acknowledgments

The authors thank two reviewers for their numerous constructive comments and suggestions that helped to improve the paper significantly. This work is partially supported by NSAF (No. U1430101), the National Natural Science Foundation of China (91330106, 11571047, 11571048, 11401034), China Postdoctoral Science Foundation (20110490328), the natural science foundation of Shandong Province (ZR2012AM019, ZR2013AM023, ZR2014AM013), and Independent innovation foundation of Shandong University (2012TS018).

References

- [1] K. Lipnikov, M. Shashkov, D. Svyatskiy, Yu. Vassilevski, Monotone finite volume schemes for diffusion equations on unstructured triangular and shape-regular polygonal meshes, *J. Comput. Phys.* 227, 492-512 (2007).
- [2] I. Aavatsmark, An introduction to multipoint flux approximations for quadrilateral grids, *Comput. Geosci.* 6, 405-432 (2002).
- [3] I. Aavatsmark, T. Barkve, O. Boe, T. Mannseth, Discretization on unstructured grids for inhomogeneous, anisotropic media Part I: Derivation of the methods. *SIAM J. Sci. Comput.* 19, 1700-1716 (1998).
- [4] Zhiqiang Sheng and Guangwei Yuan, A nine point scheme for the approximation of diffusion operators on distorted quadrilateral meshes. *SIAM J. Sci. Comput.* 30, 1341-1361 (2008).
- [5] L. Chang, G. Yuan, Cell-centered finite volume methods with flexible stencils for diffusion equations on general nonconforming meshes, *Comput. Methods Appl. Mech. Engrg.* 198, 1638-1646 (2009).
- [6] Jingming Wu, Zihuan Dai, Zhiming Gao, Guangwei Yuan, Linearity preserving nine-point schemes for diffusion equation on distorted quadrilateral meshes, *J. Comput. Phys.* 229, 3382-3401 (2010).
- [7] S. Korotov, M. Krizek, P. Neittaanmi, Weakened acute type condition for tetrahedral triangulations and the discrete maximum principle, *Math. Comput.* 70, 107-119 (2000).
- [8] I.D. Mishev, Finite volume methods on Voronoi meshes, *Numer. Methods PDEs.* 12, 193-212 (1998).
- [9] Eirik Keilegarnen, Jan M. Nordbotten, Ivar Aavatsmark, Sufficient criteria are necessary for monotone control volume methods, *Appl. Math. Lett.* 22, 1178-1180 (2009).
- [10] J. M. Nordbotten, I. Aavatsmark, G. T. Eigestad, Monotonicity of control volume methods, *Numer. Math.* 106, 255-288 (2007).

- [11] E. Keilegarlen, I. Aavatsmark, Monotonicity for MPFA methods on triangular grids, *Comput. Geosci.* 15, 3-16 (2011).
- [12] Michael G. Edwards, Hongwen Zheng, Double-families of quasi-positive Darcy-flux approximations with highly anisotropic tensors on structured and unstructured grids, *J. Comput. Phys.* 229, 594-625 (2010).
- [13] Michael G. Edwards and Hongwen Zheng, A quasi-positive family of continuous Darcy-flux finite-volume schemes with full pressure support. *J. Comput. Phys.* 227, 9333-9364 (2008).
- [14] K. Lipnikov, G. Manzini, and D. Svyatskiy, Analysis of the monotonicity conditions in the mimetic finite difference method for elliptic problems, *J. Comput. Phys.* 230, 2620-2642 (2011).
- [15] K. Lipnikov, G. Manzini, and D. Svyatskiy, Monotonocity conditions in the mimetic finite difference method. J. Fořt et al., *Finite volumes for complex applications VI-problems & perspectives*, Springer proceedings in mathematics 4, DOI 10.1007/978-3-642-20671-9_69, ©Springer-Verlag Berlin Heidelberg 2011.
- [16] P. Sharma and G. W. Hammett, Preserving monotonicity in anisotropic diffusion, *J. Comput. Phys.* 227, 123-142 (2007).
- [17] R. Liska and M. Shashkov, Enforcing the discrete maximum principle for linear finite element solutions of second-Order elliptic problems, *Commun. Comput. Phys.* 3, 852-877 (2008).
- [18] C. Le Potier, Finite volume monotone scheme for highly anisotropic diffusion operators on unstructured triangular meshes, *C. R. Acad. Sci.Paris Ser.I.* 341, 787-792 (2005).
- [19] Guangwei Yuan, Zhiqiang Sheng, Monotone finite volume schemes for diffusion equations on polygonal meshes, *J. Comput. Phys.* 227, 6288-6312 (2008).
- [20] Zhiqiang Sheng, Guangwei Yuan, The finite volume scheme preserving extremum principle for diffusion equations on polygonal meshes, *J. Comput. Phys.* 230, 2588-2604 (2011).
- [21] K. Lipnikov, D. Svyatskiy, Y. Vassilevski, Interpolation-free monotone finite volume method for diffusion equations on polygonal meshes, *J. Comput. Phys.* 228, 703-716 (2009)
- [22] K. Lipnikov, D. Svyatskiy, Y. Vassilevski, A monotone finite volume method for advection-diffusion equations on unstructured polygonal meshes, *J. Comput. Phys.* 229, 4017-4032 (2010).
- [23] T. S. Palmer, A point-centered diffusion differencing for unstructured meshes in 3-D, UCRL-JC-118730, 1994.
- [24] Guangnan Chen, Deyuan Li, Zhengsu Wan, Difference scheme by integral interpolation method for three dimensional diffusion equation. *Chinese Journal of Computational Physics*, 20, 205-209 (2003).
- [25] Zhengping Du, Dongsheng Yin, Xiaoyu Liu, Jinfu Lu, Nonorthogonal hexahedralmesh finite volume difference method for the 3-D diffusion equation. *J Tsinghua Univ (Sci & Tech)*, 43, 1365-1368 (2003).
- [26] Dongsheng Yin, Zhengping Du, Jinfu Lu, An unstructured tetrahedral mesh finite volume difference method for the diffusion equation. *J. Numer. Methods Comput. Appl.* 2, 92-100 (2005).
- [27] K. Lipnikov, M. Shashkov, D. Svyatskiy, The mimetic finite difference discretization of diffusion problem on unstructured polyhedral meshes, *J. Comput. Phys.* 211, 473-491 (2006).
- [28] Xiang Lai, Zhiqiang Sheng and Guangwei Yuan, A Finite Volume Scheme for Three-Dimensional Diffusion Equations, *Communications in Computational Physics*, 18, 650-672 (2015).
- [29] A. Berman, R. J. Plemmons, *Nonnegative matrices in the mathematical science*, Academic

Press, New York, 1979.

- [30] Michael G. Edwards, Hongwen Zheng, Quasi M-Matrix multifamily continuous Darcy-flux approximations with full pressure support on structured and unstructured grids in three dimension, *SIAM J. Sci. Comput.* 33, 455-487 (2011).
- [31] M. Pal, M. Edwards, Continuous Darcy-flux approximation for general 3-D grids of any element type, paper SPE 106486. In: SPE Reservoir simulation symposium. Houston, Texas, USA, 26-28 February 2007.
- [32] I. V. Kapyrin, A family of monotone methods for the numerical solution of three-dimensional diffusion problems on unstructured tetrahedral meshes, *Mathematics*. 416, 588-593 (2007).
- [33] A. Danilov, Yu. Vassilevski. A monotone nonlinear finite volume method for diffusion equations on conformal polyhedral meshes, *Russ. J. Numer. Anal. Math. Modeling*, 24, 207-227 (2009).
- [34] K. Nikitin, Yu. Vassilevski, A monotone nonlinear finite volume method for advection-diffusion equations on unstructured polyhedral meshes in 3D, *Russ. J. Numer. Anal. Math. Modelling*, 25, 335-358 (2010).